Solar Energy 271 (2024) 112446

Contents lists available at ScienceDirect

Solar Energy

journal homepage: www.elsevier.com/locate/solener

Assessment of the impact of utility-scale photovoltaics on the surrounding environment in the Iberian Peninsula. Alternatives for the coexistence with agriculture

Miguel-Ángel Muñoz-García [a,*], Luis Fialho [b], Guillermo P. Moreda [a], Fátima Baptista [b]

[a] Universidad Politécnica de Madrid, Dep. Ing. Agroforestal, ETSIAAB, LPF-TAGRALIA, Av. Puerta de Hierro, 2, 28040 Madrid, Spain

[b] MED - Instituto Mediterrâneo para a Agricultura, Ambiente e Desenvolvimento, Universidade de Évora and Cátedra de Energia Renováveis, Pólo da Mitra, Ap. 94, 7006-554 Évora, Portugal

ARTICLE INFO

Keywords:
Agrivoltaics
Ground-integrated photovoltaics
Photovoltaics
Remote sensing
Satellite images

ABSTRACT

The rapid growth of photovoltaic solar energy, to achieve decarbonization, has been accompanied by increasing land occupation and the subsequent concern in the agroforestry sector. The increase in land area occupied has been of 20% in recent years, boosting solar electricity production to 5.9% of the total in Europe. This fact raises the question of the impact on vegetation greenness and moisture in the rural environment, something that has not always been considered.

Image analysis is presented as one of the most effective tools to estimate the variation of vegetation greenness and moisture. For this, terrestrial images, like those from unmanned aerial vehicles, can be used; however, this limits the amount of information available and/or increases the cost. The use of satellite images in different bands is a relatively new tool that can be exploited for the analysis of solar plants impact. This work presents a new way to use Sentinel imagery to analyse the impact of utility-scale solar plants on vegetation and moisture of the surrounding areas. According to our results, a moderate decrease in weighted index for both moisture (5%) and vegetation (3%) occurred after solar plant installation. It is expected that these results can be of help for the design of new PV and agrivoltaic plants, originating the Ground-Integrated Photovoltaics (GIPV).

1. Introduction

The growth of photovoltaic solar energy has been unstoppable in the last decades, and more accelerated yet in recent years. The electric energy demand, together with the decarbonization strategy of most countries, is causing the demand of photovoltaic solar energy to skyrocket [1]. According to the International Energy Agency, electricity demand is forecasted to grow at an annual rate of 3 % over the next three years compared to 2022 [2,3], with one-third of the global consumption located in China. Besides, more than one-third of the world's electricity consumption will come from renewables in 2025 [3]. Such contribution entails that CO_2 emissions are still growing, but more slowly than in former years, making renewable energies the way to reach the net-zero emissions goal.

Global electricity consumption grew from about 11,000 TWh in 1990 to more than 26,000 TWh in 2022. Even the global energetic crisis caused by the war in Ukraine made global electricity demand growth slow-down only slightly in 2022. Renewable energies as a whole are the main growing energy source, with around 400 TWh of increase in the period from 2019 to 2022. Even the initial forecast for the growth in 2023 has been overpassed and renewable energies had grown more than 1000 TWh at mid-2023.

Photovoltaics (PV) is among the cheapest ways to produce electricity, due to the descent in the price of the main element: the solar panel. Nonetheless, the success of PV has also brought criticism [4], not always based on scientific evidence and often pushed by spurious interests. Regardless of the reasons behind criticism, the occupation of the land by ground-mounted PV plants is a fact to be considered. The best scenario for the installation of photovoltaic plants would be the use of unproductive land. Nonetheless, in a context of ever-growing world population and the subsequent food demand, there is the possibility of coexistence or land sharing between PV and agriculture, recently coined

* Corresponding author at: Universidad Politécnica de Madrid, Dep. Ing. Agroforestal-Electrotecnia y Energías Renovables, LPF-TAGRALIA, Avda. Complutense s/n, 28040 Madrid, Spain.

E-mail address: miguelangel.munoz@upm.es (M.-Á. Muñoz-García).

https://doi.org/10.1016/j.solener.2024.112446
Received 8 January 2024; Received in revised form 28 February 2024; Accepted 3 March 2024
Available online 12 March 2024

with the terms Agri-photovoltaics, Agrivoltaics or Agrovoltaics (APV) [5].

In the scientific literature, there are many works that deal with building integrated photovoltaics (BIPV). Photovoltaic integration in buildings arises from the need to improve the aesthetics of photovoltaic systems, without this necessarily implying a reduction in electricity production. It is a concept that occupies entire sections in world congresses and that is fully accepted. Likewise, there are works that address the aesthetic issues of large ground-mounted photovoltaic plants in the countryside. Some of these works call this strategy Land Integrated Photovoltaics (LIPV) [4], looking for a visual harmony of the panels with the surrounding landscape.

Here, we propose to extend the LIPV concept to agriculture, since land integration alone does not consider if the previous (or potential) crop in the land is maintained or integrated when the solar plant is designed and installed. In this case, not only the land but also the soil, understood as the substrate for the crop, should be considered and so the BIPV appears as an extension of LIPV. According to Elkadeem et al. (2024) [6], despite not all the land is suitable for the combined PV-agriculture use, at least 8 % is, in countries like Sweden.

Lately in the Iberian Peninsula, the capacity of new grid-connected ground-mounted PV power plants has evolved from small and medium 'solar farms' to large utility-scale plants. Following the US National Renewable Energies Laboratory, the term 'utility-scale' is for capacities greater than 5 MWp. Although there are examples of utility-scale power plants that harness other solar technologies like thermoelectric, the vast majority of the capacity installed in the last years in the Iberian Peninsula is solar PV.

In parallel with the deployment of utility-scale PV power plants, concern has been raised about their side-effects on native vegetation and wildlife, on local and regional climate and, in a nutshell, on ecosystem services (Randle-Boggis et al., 2020) [7]. With regards to effect on local climate, the model proposed by Hu et al. (2016) [8] envisaged PV plant local cooling of about -2 °C, while the simulation conducted by Millstein and Menon (2011) [9] concluded that extensive adoption of PV in desert areas of USA would lead to a significant local temperature increase of + 0.4 °C. Chang et al. (2022) [10] developed a land-surface energy balance model for PV plants of fix tilt angle which was subsequently incorporated into a meteorological model. After comparing with field observations from two utility-scale PV plants, they concluded that the resulting model reproduced accurately the temporal pattern of maximum daily temperature and land surface temperature (LST). Other researchers have installed air temperature sensors within the boundaries of the PV plant as well as in its vicinity taken as the control. For instance, Barron-Gafford et al. (2016) [11] found that the local nighttime temperature over a PV plant was regularly 3.5 °C warmer than the control wildland, which supported the hypothesis of an urban-like heat island effect associated to PV power plant. Nevertheless, their result could have been affected by convection from a nearby parking lot, as pointed by Broadbent et al. (2019) [12]. The latter authors reported average daytime air temperature 1.3 °C warmer than the reference site, although they stated that factors like wind speed and cloud cover played a role. On the other hand, Broadbent et al. (2019) [12] found no significant difference in nighttime air temperature between the plant and the reference site, unlike Barron-Gafford et al. (2016) [11].

Unlike the effect of PV plants on local air temperature, the amount of research about ecohydrological effects of utility-scale PV plants on their surrounding environment is limited (Wu et al., 2022 [13]; Yavari et al., 2022 [14]). Armstrong et al. (2016) [15] reported lower daily maximum absolute humidity under the PV arrays, which suggested lower evapotranspiration rates. Choi et al. (2023) [16] reported significantly higher soil moisture in vegetated PV arrays compared to conventional bare PV soil. They suggested that higher soil temperature could be in part responsible for the lower soil moisture in the bare PV. Kannenberg et al. (2023) [17] found minimal impact of a single-axis tracking PV array on APV grassland evapotranspiration and productivity, despite the shade casted by the PV panels. They suggested that the dynamic tilt angle resulted in more uniform soil wetting compared to fix tilt angle arrays, where moisture intercepted by the panels drips across the same edge. Li et al. (2018) [18] used a climate model to determine the effects of covering 20 % of the Sahara Desert land with PV panels on rain. Their simulations showed that a 50 % increase in precipitation (+0.13 mm/day) could be expected.

Barron-Gafford et al. (2016) and Guoqing et al. (2021) [19] mentioned the need to consider the impacts of utility-scale PV plants beyond their boundaries, and how they affect to surrounding land use management. As a rule of thumb, no previous in-field data of LST, soil moisture or near-surface air temperature will be available for the specific site where a PV plant has been installed. LST, as well as the normalized difference moisture index (NDMI), the normalized difference vegetation index (NDVI), and other vegetation indices, can be derived from remote sensing data, i.e. Earth observation satellite images. To analyse the potential impact of PV plant installation on the surrounding environment, these images are a valuable resource, since they are available not only for after PV plant installation dates, but also before (Guoqing et al., 2021; Hurduc et al., 2024).

From the foregoing literature review it follows that a number of works addressed the effect of PV plant on air temperature, some fewer tackled the effects on rain and soil moisture, and very few dealt with the impact on surrounding vegetation. The latter knowledge gap pushed us to undertake the present study.

1.1. Objectives

The land area dedicated to PV power plants has increased exponentially in recent years. Our study seeks to determine land use scenarios that fulfil the EU objectives. We intend to give answer to three questions:

- How can satellite images be exploited to analyse the impact of utility-scale PV plants?
- What is an effective method to determine environmental variables related to a PV solar plant from satellite images?
- Which is the environmental impact of the installation of a solar plant on the surrounding land, and what mitigating measures can be adopted?

2. Materials and methods

With the aim of determining the real impact that the installation of large photovoltaic plants has on the environment, a test was planned based on the analysis of satellite images, using data from the Copernicus mission. The Iberian Peninsula was selected for the analysis due to its character of privileged European region in terms of solar radiation and therefore an unbeatable place for the installation of large photovoltaic plants. Eight large PV plants (unit acreage greater than 50 ha) were selected, six of them located in Spain and the other two located in Portugal.

The starting data are satellite images, both those provided by Google Maps, to locate large photovoltaic plants, determining whether they have been installed in recent years, as well as those provided by the Sentinel mission. In both cases these are free access images, considered sufficient for the purpose of this work.

The methodology used is based on the temporal analysis of the image data in the frequency bands that provide the vegetation and moisture indices in the areas surrounding the solar plants, as well as in the areas internal to them, excluding the surface occupied by the photovoltaic panels. The following sections explain in detail the criteria for selecting the images, the type of image used, and the method devised to eliminate the dependence of the variation of the moisture and vegetation indices with respect to the weather of the year.

2.1. Satellite images to analyse the impact of utility-scale PV power plants

Copernicus Sentinel missions are an EU project launched for scientific purposes based on twin satellites that give name to the different Sentinel missions. Sentinel-2 and Sentinel-3 missions, were used in this study, depending on the resolution required. Previous works have used Sentinel for PV related tasks such as site selection (Demir et al., 2023) [20]. In this work, Sentinel images were used to assess the impact of photovoltaic plants on the vegetation in these areas.

Sentinel-2 provides access to 12 bands, and the methodology proposed is the result for different tests by combining bands and data processing. Two levels of data processing are provided by Sentinel: Since Level1 does not correct the effects of the atmosphere, we used Level2 data, where the effects of the atmosphere on the light that is reflected off the surface of the Earth and reaches the sensor are excluded. Data are available globally since March 2017.

Image resolution of Sentinel-2 is presented in Annex 1.

Sentinel-3 mission has an Instrument Payload dedicated to different scientific areas:

- Ocean and Land Colour Instrument (OLCI),
- Sea and Land Surface Temperature Radiometer (SLSTR),
- SAR Radar Altimeter (SRAL),
- MicroWave Radiometer (MWR).
- Precise Orbit Determination (POD) instruments.

Image resolution of Sentinel-3 OLCI is presented in Annex 1.

Other researchers have used Sentinel-2 images for the assessment of PV installations (Zhang et al., 2023) [21], with different intentions. In the aforementioned case, the aim was to determine the coverage by panels in certain areas, something that we have also done in this work. However, in our case we have removed the influence of the panels on the image to determine the remaining environmental impact.

Once the solar plants were identified (Table 1 and Fig. 1), two images of each plant were collected from Copernicus in dry and wet seasons. Also, images were obtained both before and after the solar plant installation. The days selected were based on the availability of clear images (less than 20 % cloudy), so they were not necessarily the same day but as close to as possible.

The years selected fulfilled the condition of being similar hydrological years. According to AEMET, the hydrological years 2017/18 and 2022/23 were both dry and similar in terms of rainfall (474 mm and 487 mm, respectively).

Table 1
The eight PV plants or solar plants (SP) analysed.

Code	Country	Type of tracking	Sloped terrain (yes for slope > 10 %)	Occupation (**ha**)
SP1	Spain	Horizontal single-axis	No (average grade lower than 2 %)	820
SP2	Spain	No tracking (fix tilt angle of 20°)	No (average grade lower than 3 %)	300
SP3	Portugal	Fix, ground oriented	Yes (grades up to ca. 58 %)	100
SP4	Spain	No tracking (fix tilt)	No (average grade lower than 3.5 %)	943
SP5	Spain	No tracking (fix tilt)	Yes (average grade lower than 12 %)	1000
SP6	Spain	Horizontal single-axis	No (average grade lower than 1 %); But ends where a hill starts	28.35
SP7	Spain	No tracking (fix tilt)	Not in the solar plant. But the plant ends near hills	100 MWp
SP8	Portugal	No tracking (fix tilt)	No (average grade lower than 6 %)	368

The study used 144 satellite images in total. For each PV plant, 18 satellite images were exploited, including two seasons (dry or summer, wet or spring) and different band combinations, as well as different scenarios of the use of land. It must be noted that in general the surrounding lands also experimented changes, mainly due to the agricultural use depending on the crop, tillage practices, land management, etc. Farther on it is explained how to exclude as much as possible the influence of third-party activities apart from the solar plant.

2.2. Validation of the selected images

To follow an objective and reproducible analytic method, besides using two periods of the year before and after the installation, the NDVI and NDMI images obtained from Sentinel, were processed with ImageJ, a public domain Java image processing software. The objective was to compare the vegetation cover before and after the installation as an index of the environmental and agronomical impacts.

It was considered that, given that these are large PV plants, and that Sentinel presents a limited resolution, a mechanism that would eliminate the influence of other external factors, should be used. Then, it was considered an expanded area (100 times larger), for which the area of the photovoltaic plant is not significant (<1%). The 2017 and 2023 vegetation indices were then compared for this expanded area, and show an average reduction of 5 %, regardless of the existence of a photovoltaic plant.

Therefore, to eliminate the influence of climate change, vegetation in the area where the photovoltaic plant is located was not compared, but vegetation in the area where no photovoltaic plant is located was compared (2017 to 2023). This process was carried out independently for each photovoltaic plant for 2017 and 2023.

Finally, these relative indices were compared to determine if there is relative variation between both years.

It must be pointed out that, to minimize the influence of nearby urban changes along the years considered, or local climatic effects, when images covering an encompassing area 100 times larger than the plant presented NDVI or NDMI indexes variation from 2017 to 2013 greater than 10 %, such plants were discarded.

2.3. Environmental and agronomic impacts of a solar plant by analysing vegetation and moisture indices

The use of infrared images for the analysis of defects or malfunctioning in PV modules is commonly applied to photovoltaic systems (Buerhop et al., 2022) [22]. Usually, hot spots due to defective PV modules or shading can be detected with this technology. But infrared images can also be used for the detection of vegetation and in the common NDVI reflected infrared bands can lead to an erroneous vegetation index determination. Nevertheless, combining different bands (Jörges et al., 2023) [23] an analysis of the impact of the solar plant can be performed. For crystalline silicon (c-Si) based PV modules, the reflectance presents an increase from 990 nm to 1150 nm. In Annex-I, the detailed bands provided by Copernicus Sentinel-2 program are presented. Bands 9 and 10 are the closest to such reflectance window. An example of the NDVI images used is in Fig. 2.

Besides NDVI, we used the NDMI. NDMI analysis uses NIR and SWIR bands to display moisture. The SWIR band reflects changes in both the water moisture content of the vegetation and the structure of the spongy mesophyll in the vegetation canopies, while the NIR reflectance is affected by the internal structure and dry matter content of the leaf, but not by its moisture content. An example of this method is presented in Fig. 3.

Note that Figs. 2 and 3 were obtained from Sentinel-2 using the normalized color scale for NDVI and NDMI, respectively, in order to present a better visual effect. Nevertheless, the original Sentinel-2 grayscale images were used for the analysis, as stated below. We used ImageJ to calculate the NDVI and NDMI histograms whose mean values

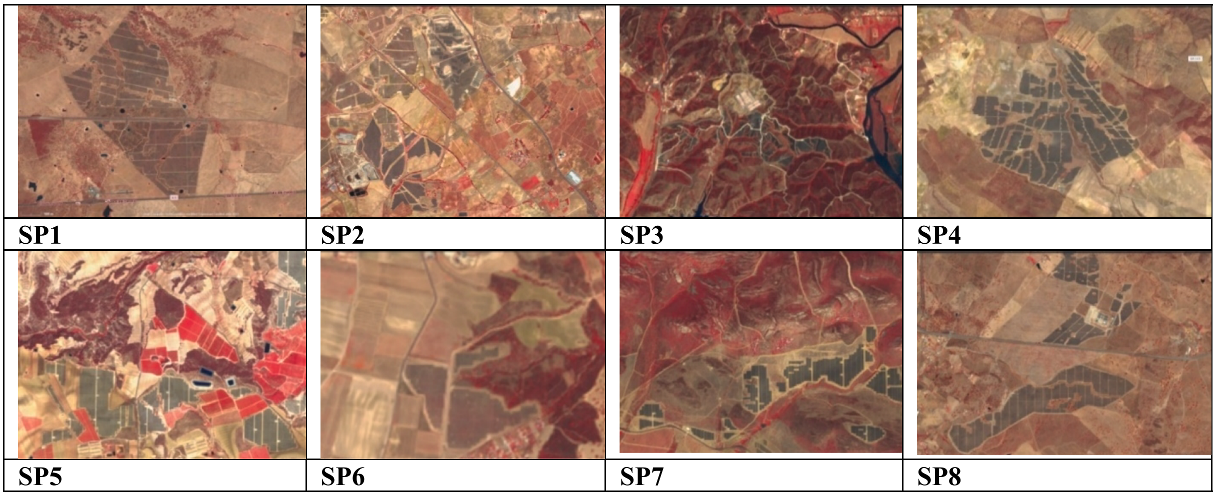

Fig. 1. Satellite false colour images for the eight solar plants (SP) analysed.

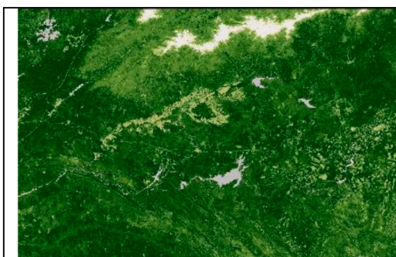	NDVI image from spring 2017 Index:190.4	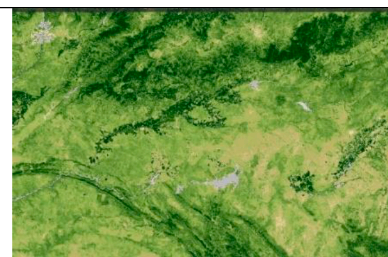	NDVI image from summer 2017 Index:157.6
	NDVI image from spring 2023 Index:185.6	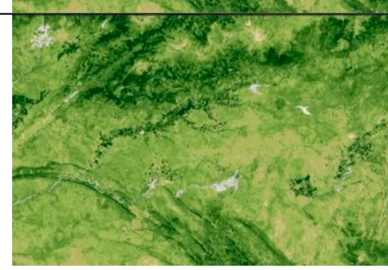	NDVI image from summer 2023 Iindex:157.1
Wide area (out). NDVI spring index variation 2023/2017	0.975	Wide area (out). NDVI summer index variation 2023/2017	0.997
NDVI mean index variation. OUT2023/OUT2017	0.986		

Fig. 2. Using NDVI images from 2017 and 2023 in the same geographic area.

were used as indices.

2.4. The use of relative indices to assess the impact of a solar plant

The method consisted of taking images of the same area with a time offset of 5 years, before and after the installation of the plant, and generating relative indices of both vegetation and humidity to eliminate the influence of meteorological changes and urban or agricultural management actions in the area.

Images that covered only the PV plant were used, along with broader images. The broader images where then compared for Summer and Spring of the two years to verify that the large area does not undergo substantial changes (due to externality factors such as climate change) and then the area surrounding the PV plant was compared before and after the plant construction, eliminating the plant itself from the image for both years and seasons.

Once the images were collected, the first step was to obtain a template through selective filtering that would allow the area covered by the PV plant to be eliminated. To do this, images with smaller aperture and false color were used (see Fig. 4a). Then, the area occupied by the PV modules was eliminated from the images, by obtaining a template with the PV modules (see Fig. 4a), both before and after the PV plant installation (see Fig. 4c–f). Afterwards, the NDMI and NDVI indices were derived by calculating the histograms. Finally, relative indices were obtained by dividing the index of the surrounding area of the plant, excluding the area of PV modules, by the index of the encompassing area, for each season (spring, summer) and year (2017 and 2023). The average value of both seasons was taken as the year index.

In short, the method followed consisted of the following steps:

- Take images NDMI and NDVI for each plant, before and after the installation of the plant, for two seasons.
- Process the images to subtract the area of the PV panels.
- Obtain the histogram as a number to be compared.
- Compare histograms of surrounding area of the solar plant and encompassing area including the solar plant

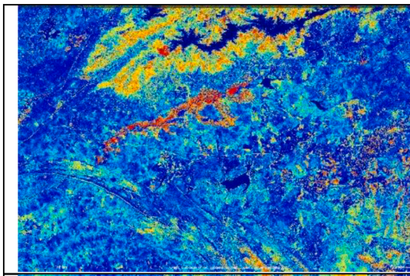	NDMI image from spring 2017 Index:145.46	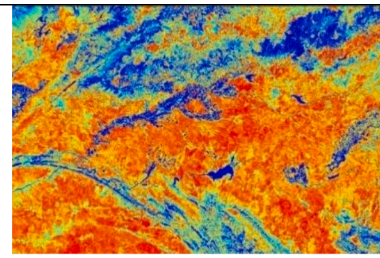	NDMI image from summer 2017 Index:117.94
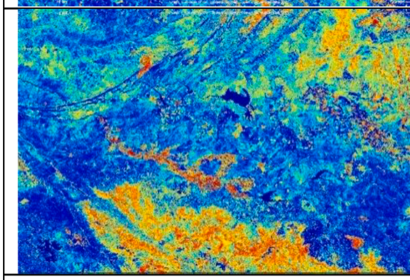	NDMI image from spring 2023 Iindex:140.57	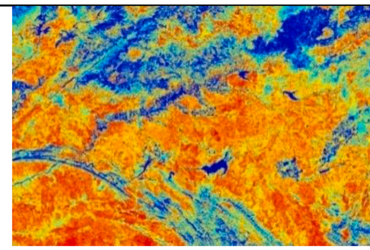	NDMI image from summer 2023 index:120.08
Wide area (out). NDMI spring index variation 2023/2017	0.966	Wide area (out). NDMI summer index variation 2023/2017	1.018
NDMI mean index variation. OUT2023/OUT2017	0.992		

Fig. 3. Using NDMI images from 2017 and 2023 in the same geographic area.

- Find the index that characterizes the effect of the solar plant installation.

This procedure is summarized in Fig. 5:

3. Results and discussion

3.1. Detection of the area occupied by the solar plant

Despite cSi in PV modules typically features a reflectance increase between 990 nm and 1150 nm (Jörges et al., 2023) [23], the spatial resolution of Sentinel closer bands, namely, Band 9 (945 nm) and Band 10 (1373 nm), 60 m, was considered insufficient. Therefore, we also considered the combination of bands 8A (864 nm) and 11 (1610 nm) with a spatial resolution of 20 m.

Fan and Huang (2021) [24] used two surface products of the Moderate Resolution Imaging Spectroradiometer (MODIS) aboard the NASA Aqua satellite to examine surface emissivity and land surface temperature of six solar farms in the southwest of USA. They observed that compared to adjacent areas that had remained unaltered, the solar farm sites reduced outgoing radiances in three MODIS infrared bands.

To date, much of the research conducted to ascertain the effect of utility-scale PV plants on local climate has focused on semiarid and arid sites of the USA (Barron-Gafford et al., 2016 [11]; Broadbent et al., 2019 [12]) and China (Wu et al., 2022 [13]; Chang et al., 2022 [10]). In contrast, the PV plants analyzed in our study are located in sites which with the exception of plant SP5, are less arid (Main climate group C – temperate, Köppen–Geiger climate classification).

Different choices for the primary colours red (R), green (G) and blue (B) were tested. Despite colour is not determinant for boundary detection, it makes easier to identify the boundaries to the unaided eye. To ease boundaries detection of the areas under supervision, visible B2 band and Long Wave Infrared B12 band were added to form the so-called false colour. With the help of the program ImageJ and its tool for filtering, using hue, saturation and brightness (HSB) color threshold, a mask for the area covered only for the PV modules is obtained. This mask was used to eliminate PV modules from the images. All the masks obtained are displayed in Fig. 6.

3.2. Environmental impact assessment: Moisture affection

To determine any effects of the solar plant on the moisture of the surrounding area, combinations of the satellite bands related to the moisture were considered. Since the PV module is a flat surface free of water (except on a rainy day and neglecting atmospheric dew condensation), the NDMI was used, which is calculated by Sentinel-2 from the B8A and B11 bands through the following equation:

NDMI = (B8A - B11) / (B8A + B11).

3.2.1. Independence and validation of the data obtained

To determine the validity of the data and to ensure the independence of the effect of the plant with respect to other effects such as changes in rainfall from one year to the next or changes in nearby agricultural management strategies, a comparison of the moisture levels of the extended area was first performed. The years 2017 and 2023 were compared, in the Spring and Summer, obtaining results like those shown in Table 2.

Data on Table 2 show how in the wide surrounding of all the plants, except SP6, there is a generalized reduction in the moisture levels detected. Given the size of the image (100 times greater than the plant image), this is not attributable to the plant, but to the fact that between the two years there is a slight drop in humidity. To discard areas where the variation in indices was very high and therefore attributable to local elements, the variation limit between 2017 and 2023 was set at 10 %. Therefore, analyses in areas with a global variation of indices of less than 10 % were considered significant, with it being very significant if it is less than 5 %. Therefore, we have eight significant cases (all) and four very significant cases (SP1, SP3, SP5, SP6) out of the total of eight. In addition to choosing only large areas with variation of less than 10 %, in this study we added one more criterion to separate the variations from external variables such as climate. To do this, what we calculate is a relative variation index between the area close to the plant and the extended area.

Fig. 7 presents graphically the data of Table 2. A ratio of 1 (100 %) means the same moisture index in both years. It can be observed that the greatest differences occur in Spring, despite in Summer the moisture levels are similar in both years for all the PV plants. Only plants SP7 and SP8 show a larger decrease (84–85 %) in Spring compared to the rest

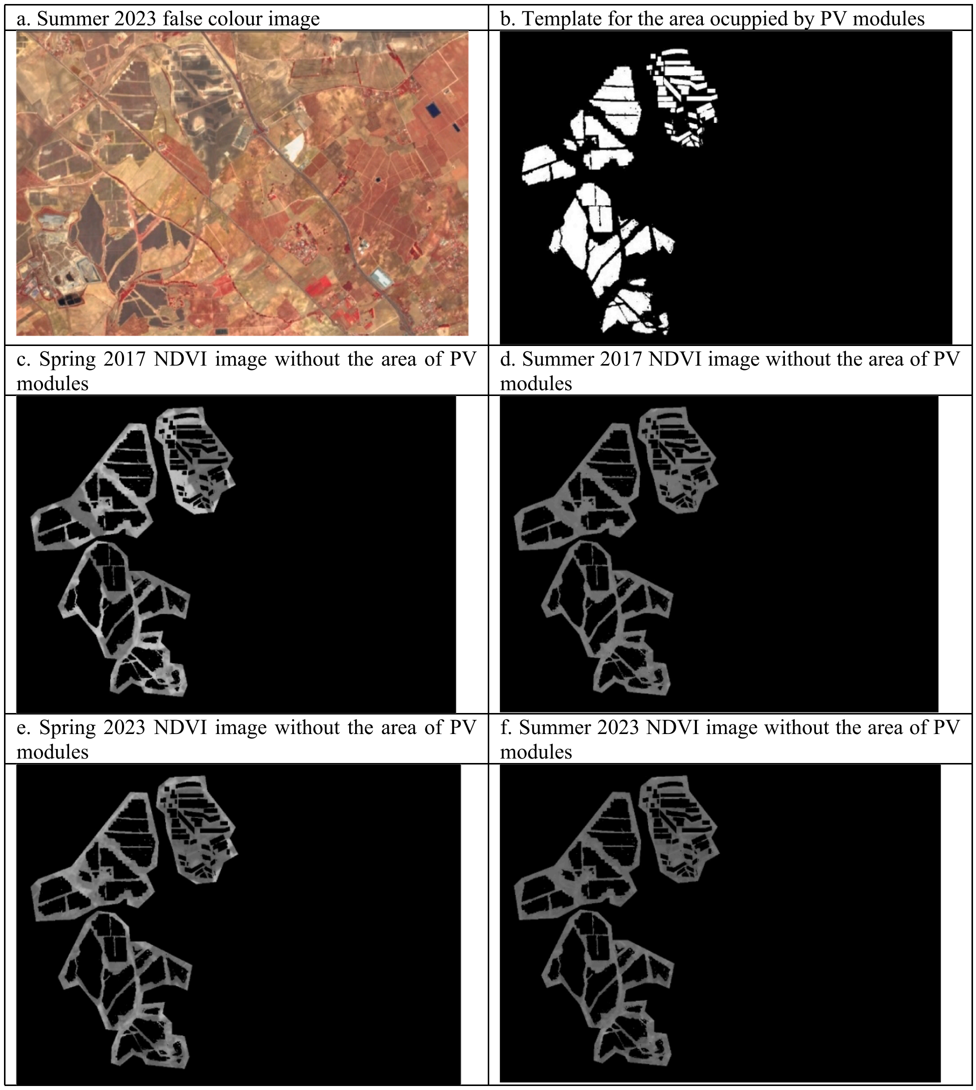

Fig. 4. Obtaining the images for the calculation of NDMI indices. Note that despite the NDMI value was higher in 2017, it must be taken as a relative index compared with the encompassing area images.

(92–100 %).

We decided to consider the very significant cases to support the main conclusions, but also the significant cases to suggest future work in the line of determining if there could be a stronger relationship, since as mentioned above, the index compares the solar plant with the surrounding area.

3.2.2. *Comparison of in/out NDMI as an index for the evaluation*

When the plant inside area, after eliminating the area occupied by the panels from the image, is compared with the outside area that encompasses the plant, in particular corresponding to a tenfold area magnification, a figure is obtained that is independent of the hydrology of the year; rather, it refers exclusively to the effect of the solar plant.

To obtain an index that is totally independent of the plant location, the inside/outside NDMI index computed from the histogram aforementioned was normalized to refer it to the condition of the initial year (2017). In this manner, it was possible to verify the evolution of the moisture relationship between the PV plant inside and outside over the time lapse studied.

According to the results depicted in Fig. 8, after the solar plant installation, the moisture index, taken as the mean of the NDMI index in the area of the solar plant, compared to the encompassing area, decreases compared to the same index before installation.

Fig. 8A) and the mean values in Table 3 show the decreasing tendency of the general moisture values. It must be noted that such data should not be mixed with the data of the encompassing area moisture indices, as in the first case we are presenting a relative index: In/out means SP area relative to the encompassing area. Thus, considering that the NDMI values decreased slightly from 2017 to 2023, this in/out index implies that in moisture decrease is higher for the PV plant inside area.

Seasonal comparisons deliver interesting results as well. First, for all the PV plants (except SP4 and SP7) the reduction was more pronounced in Spring than in Summer. Moreover, the variation in Spring was different for each plant, ranging from 2 % (SP7) to 10 % (SP2), and the summer variations were more similar for every PV plant, despite in Summer the relative NDMI indices even showed an increase in the PV plant area compared to the encompassing area. The differences observed could be associated with the slope of the terrain, that was higher for SP3 and SP5; and it was these PV plants that presented a higher value of the mean descent.

3.3. *Agronomical impact assessment: Effects on vegetation*

To evaluate the impact on vegetation, we analysed the degree of variation of the vegetated area in the zone directly influenced by the PV plant. For this purpose, the NDVI was used. Sentinel-2 calculates it from

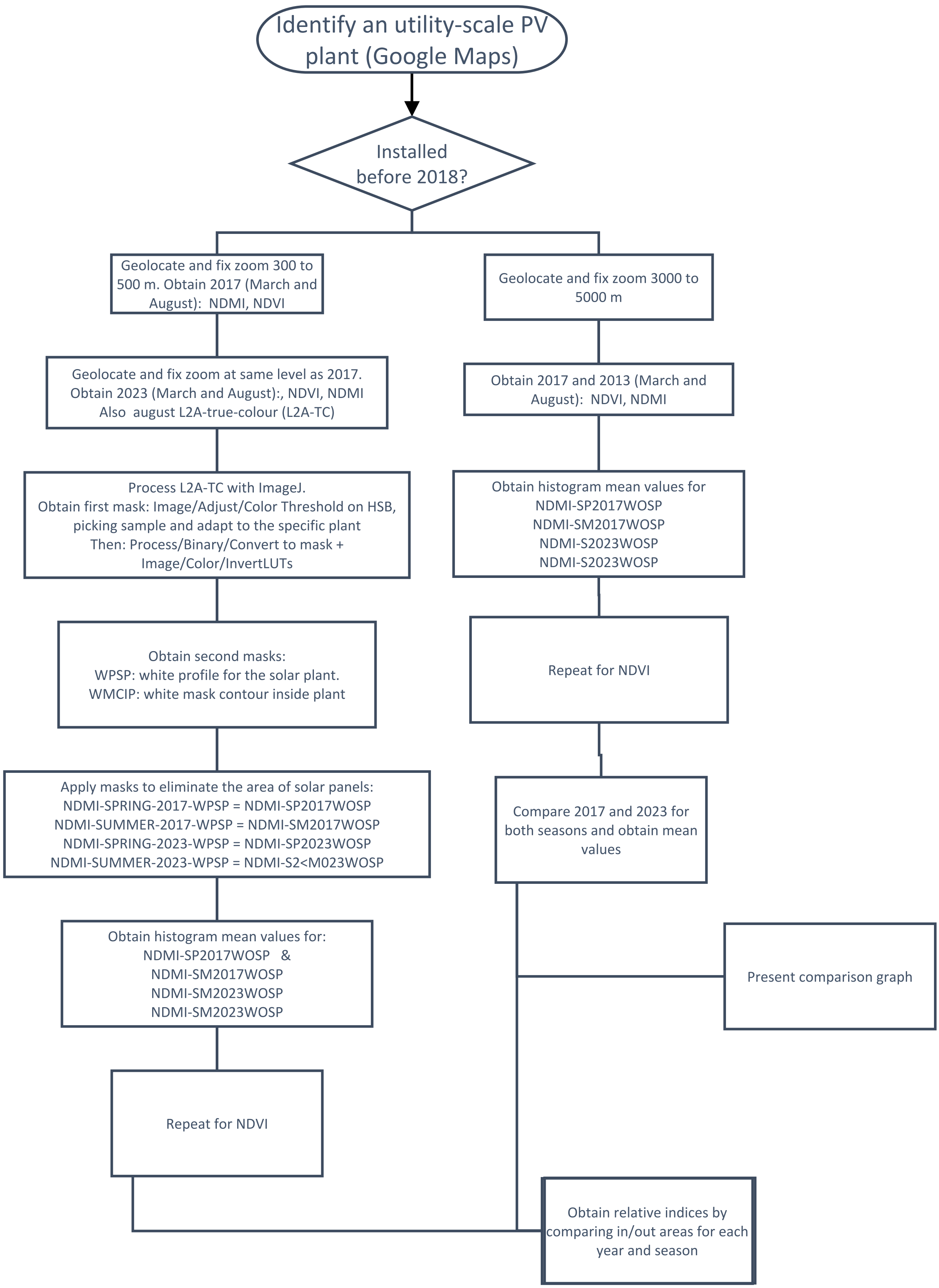

Fig. 5. Flux diagram of the process used for the analysis.

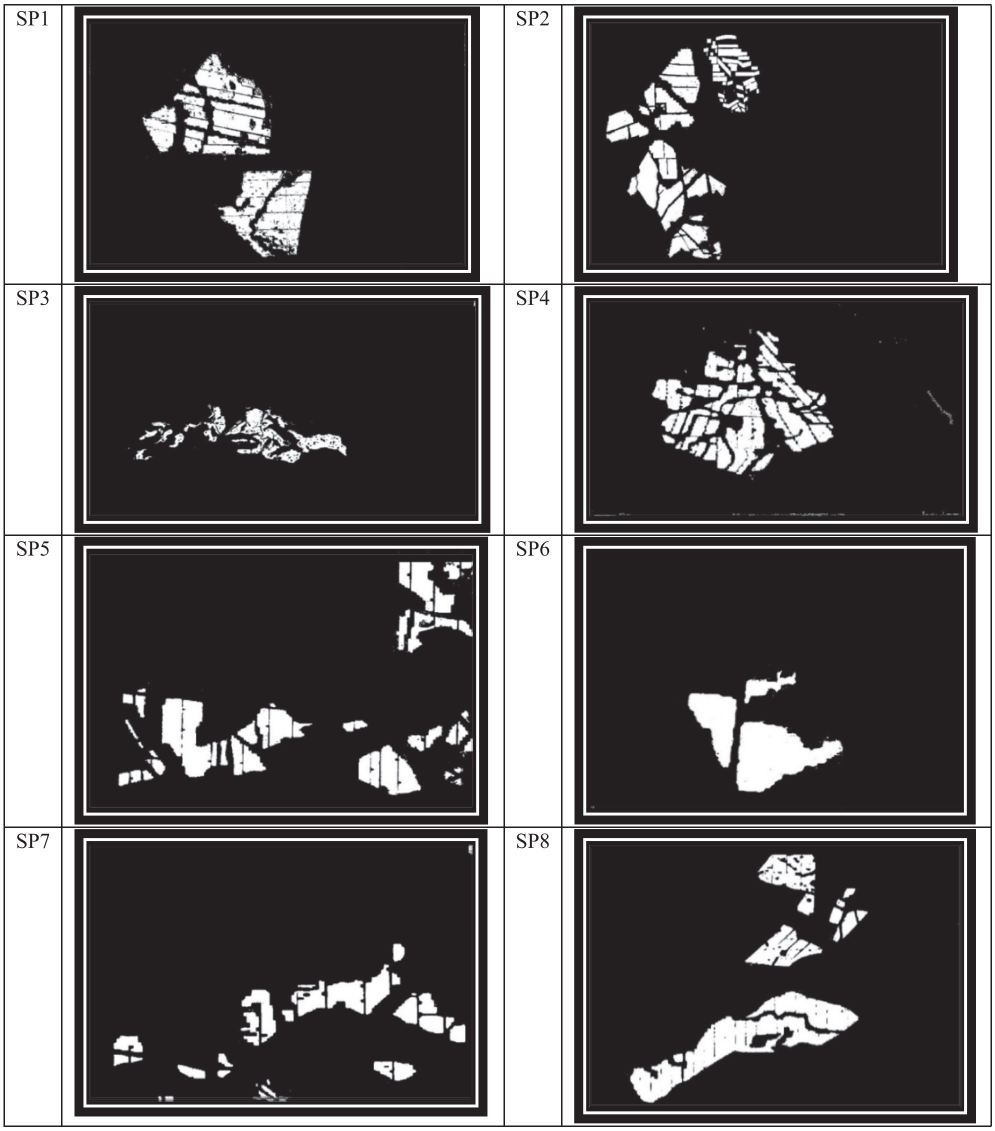

Fig. 6. Masks obtained for the solar plants analysed.

Table 2
Comparison between 2023 and 2017 histogram mean value of NDMI images for the solar plants (SP) encompassing area, for two seasons and the annual values.

NDMI in the wide area	SP1	SP2	SP3	SP4	SP5	SP6	SP7	SP8	Mean
OUT/OUT Spring23-17	0,97	0,94	0,96	0,92	0,93	1,00	0,84	0,85	0,93
OUT/OUT Summer23-17	1,02	0,90	0,97	0,97	0,99	1,01	0,97	0,96	0,97
Annual OUT/OUT 23/17	0,99	0,92	0,96	0,94	0,96	1,01	0,91	0,91	0,95

the B08 (near infrared) and B4 (red) bands as:

NDVI = (B08 – B4) / (B08 + B4).

3.3.1. Independence and validation of the obtained data

An analysis of the variation of vegetation in the PV plant encircling area was carried out, covering an area 100 times larger than that of the plant itself. It makes the influence of the solar plant negligible as it occupies less than 1 % of the covered surface, as summarized in Table 4.

For NDVI, the variation from 2017 to 2023 is even lower than for NDMI. Thus, from 2017 to 2023 there was a slight average variation in the vegetation in general, with only three cases that exhibited an average decrease greater than 5 %, but in all cases lesser than 10 %. Therefore, applying the same criterion for NDVI (vegetation analysis) than the applied for then NDMI (moisture) analysis) abovementioned.

Moreover, in this case, there were two plants for which a slight increase in vegetation was observed in the extended area, between 2017 and 2023. Anyway, the average variations were small, as corresponds to similar hydrological years.

Fig. 9 shows that, except for plants SP2, SP7 and SP8, the variation of vegetation in the encircling area is not substantial. This fact makes the further findings about the variation of vegetation inside the PV plant independent from the climate change. But even when the variation of vegetation was higher in the encompassing area, a relative index was used to avoid such influence.

3.3.2. Comparison of inside/outside NDVI as an evaluation index

In the case of vegetation indices, there was an additional pitfall due to the reflection indices of the PV panels itself. For this reason, the area

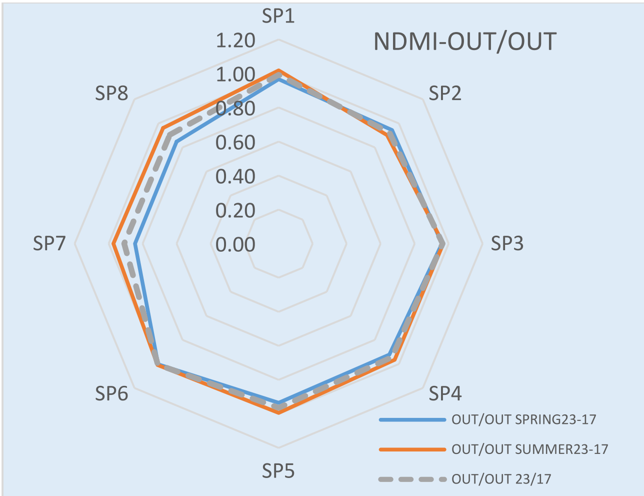

Fig. 7. Variation of NDMI from 2017 to 2023 in the encompassing area for solar plants SP1 to SP8.

occupied by the PV plant was eliminated to avoid the influence of the panels on the image.

The results indicate that both NDVI and NDMI decreased in the outside areas close to the solar plants. Hence it can be inferred that there is a slight decrease in vegetation in the surrounding environment. This may be due to the construction of roads and highways and the use of clearing and herbicides inside the plant boundary. But it could also mean

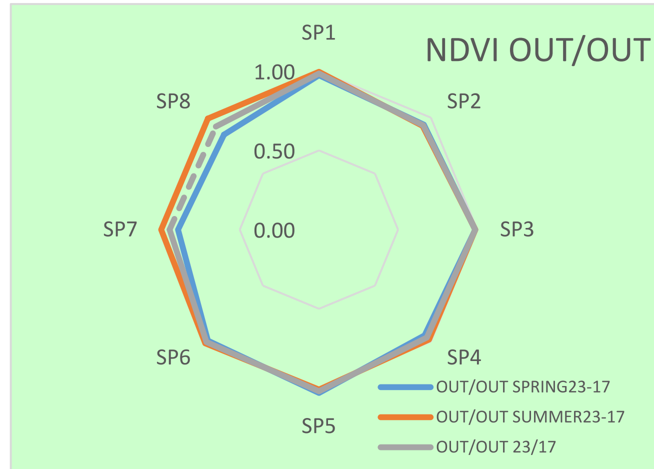

Fig. 9. Variation of NDVI from 2017 to 2023 in the encompassing area for solar plants 1 to 8.

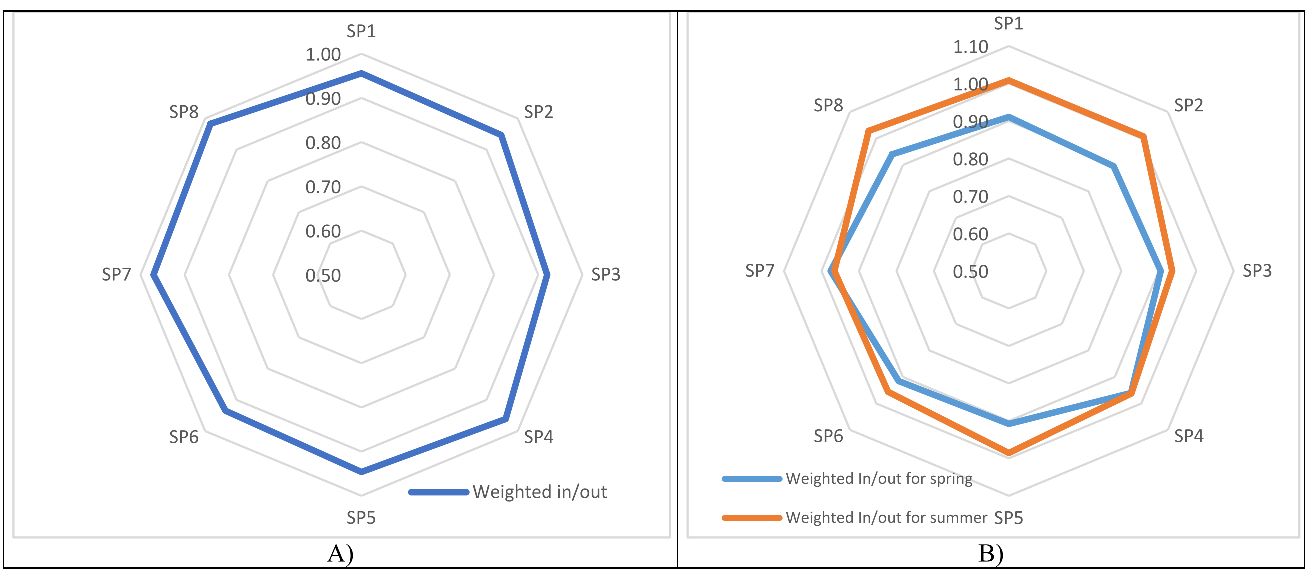

Fig. 8. Variation of the NDMI, for the area of each PV plant relative to the encompassing area, and for 2023 relative to 2017. A) displays the mean values, while B) displays the seasonal values.

Table 3
Comparison of NDMI values in solar plants (SP) area vs. the encompassing area for different seasons of 2023 vs. 2017and the mean value.

NDMI in the SP area vs. the encompassing area, 2023 vs. 2017	SP1	SP2	SP3	SP4	SP5	SP6	SP7	SP8	Mean
Weighted In/out for Spring	0,911	0,895	0,905	0,961	0,908	0,916	0,976	0,940	0,926
Weighted In/out for Summer	1,008	1,007	0,936	0,962	0,986	0,956	0,966	1,029	0,981
Annual weighted in/out	0,960	0,951	0,921	0,961	0,947	0,936	0,971	0,984	0,954

Table 4
Comparison of NDVI values for the encompassing areas.

NDVI	SP1	SP2	SP3	SP4	SP5	SP6	SP7	SP8	Mean
Out/Out Spring23-17	0.97	0.94	0.99	0.94	1.03	0.99	0.89	0.85	0.95
Out/Out Summer23-17	1.00	0.93	0.99	0.98	1.01	1.02	1.00	0.99	0.99
Annual Out/Out 23/17	0.99	0.93	0.99	0.96	1.02	1.00	0.94	0.92	0.97

that the nearby vegetation is affected, although the variations are not great.

Only for the SP5 plant the variation detected is greater, reaching an average decrease of 7 %, as shown in Fig. 10.

The average value of vegetation indices descent, obtained by comparing the plant nearness and farther area, is 2 %, when the area occupied by the panels was excluded from the analysis (see Table 5). Zhang et al. (2023) [21] found that NDVI increased after the installation of PV plants in temperate coastal zones of China but also decreased on the rest of regions. However, in our case there were plants that did not show an appreciable variation, like SP4, and others whose variation is 7 %, like SP5. In SP5, the panels are installed in an area with an orographic slope, the same as in the SP3 plant with a similar variation. Thereby, land slope could be a factor that negatively affects vegetation after the installation of a solar plant.

The data on the variation of vegetation indices led us to conclude that although the PV plant does not cause a great impact on the surrounding vegetation, this impact is a decrease in the NDVI.

Other researchers reported similar results. For instance, (Hurduc et al. 2024) [25] observed a decrease in wintery NDVI after the installation of a 46 MWp PV plant in Portugal, compared to the before-construction situation. On the other hand, they found little to no variation between the before and after situation during the estival season. (Xu et al. 2024) [26] also observed a decrease in the vegetation greenness indicator (in their case, the enhanced vegetation index, EVI) for 98 out of 116 solar parks located in different continents. They found that the effect on EVI was geographical and land cover dependent. For the North America sites, they reported a higher decrease in EVI at croplands (-19.1 %) compared to grasslands (-6.6 %), whereas for the East and South Asia sites the respective values were −5.8 % and −4.1 %. Regarding seasonal variations, the largest impact on vegetation at mid-latitudes occurred in summer. In contrast with our results and the aforementioned results by Hurduc et al. (2024) [25] and Xu et al. (2024) [26], Xia et al. (2022) [27] found a significant greening trend for the desert vegetation in the surroundings of utility-scale PV plants, comparing before- and after- PV plant installation.

3.4. Uncertainty and estimated error

Given the difficulty in validating comparing with *in-situ* measurements, NDVI uncertainty has to be derived theoretically. Thus, to estimate the expected NDVI uncertainty, Borgogno-Mondino et al. (2016) [28] applied the variance propagation law approach to estimate the uncertainty of the factors that affect the reflectance used for NDVI calculation. They stated that the major contribution to NDVI uncertainty comes from topographic and atmospheric factors. They explained that topography affects reflectance uncertainty due to its narrow relationship with sun incidence angle calculation. For an agricultural area in Northwest Italy, they observed that the absolute value of NDVI uncertainty in October (0.07) was higher than in September (0.05), which they attributed to the degradation effect of the sun elevation angle on reflectance and, ultimately, on NDVI. In our study, we use values from 0 to 255 instead of −1 to + 1, so the translation for the uncertainty 0.05–0.07 would be 6.37 to 8.92 in absolute values.

De Petris et al. (2023) [29] assessed average absolute theoretical NDVI uncertainty from the Sentinel-2 data for several European countries following a South-North gradient; the countries were Greece, Czech Republic, Lithuania, and Finland. For Greece, which is similar in latitude to the Iberian Peninsula, they reported an NDVI uncertainty of 0.06 in a spring month like April, and 0.05 in a summer month like July. On the other hand, De Petris et al. (2023) [29] found no significant differences in the temporal (month-wise) profile of NDVI uncertainty among the four countries aforementioned.

With regards to NDMI, if we compare the bands involved in its calculation (band 8A and band 11, Table A2) with their counterparts of NDVI (bands 4 and 8, Table A1), we observe that the values of signal-to-noise ratio (SNR) are lower for the NDMI calculation bands. Considering that the SNR is the inverse of the noise-to-signal ratio, the NDMI uncertainty is higher than NDVI uncertainty. Nevertheless, considering the SNR high values (>70), as stated before, the main factor does not come from the sensor but from external factors.

On this study, instead of absolute NDVI and NDMI values we computed relative values comparing the same images with different zoom size. Therefore, it can be expected that the effect on NDVI and NDMI uncertainty in one or another year is smaller than de variation obtained as results.

3.5. How agrivoltaics can aid to attenuate the estimated impact

According to our findings, conventional PV plants have some impact on the surrounding land environment. Probably, this is due to the fact that the roads that lead to the areas of the panels are usually weeded to facilitate the traffic of maintenance vehicles.

If an agrivoltaic system was considered, the impact on the land would be smaller, since the crop vegetation on one hand is able to maintain certain levels of moisture and also it would increase the land use efficiency so that the overall yield obtained from the land would be higher.

Agrivoltaics can also help to recover decreasing acreage for arable lands (Pulkit et al., 2021) [30] maintaining the capacity to produce foodstuffs in a scenario of world growing population. Even more, the PV plant, built under the conditions of coexistence with agriculture (Muñoz and Hernández, 2022) [31], can contribute to the improvement in the production of the solar plant itself, since the evapotranspiration of the

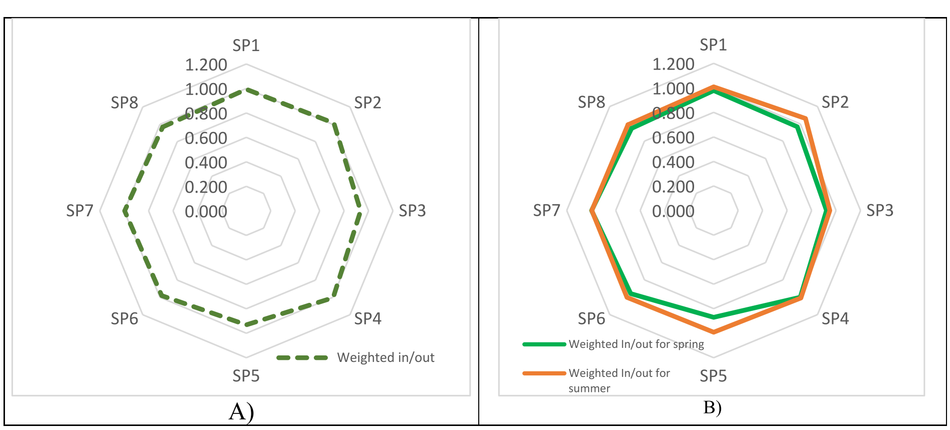

Fig. 10. Variation of NDVI for the area of each solar plant relative to the encompassing area, for 2023 relative to 2017. A) displays the mean values while B) displays the seasonal values.

Table 5
Comparison of NDVI values in solar plants area relative to the encompassing area for two seasons of 2023 vs. 2017, and the overarching mean value.

NDVI for the SP area relative to the encompassing area, 2023 relative to 2017	SP1	SP2	SP3	SP4	SP5	SP6	SP7	SP8	Mean
Weighted In/out for spring	0,978	0,966	0,922	1,000	0,871	0,958	0,997	0,948	0,955
Weighted In/out for summer	1,009	1,061	0,949	1,008	0,992	1,001	0,995	0,989	1,001
Average weighted in/out	0,994	1,014	0,935	1,004	0,931	0,980	0,996	0,969	0,978

plants contributes to lower the temperature of the solar panels, with the subsequent improvement in performance. In addition, the vegetation cover of the soil, whether due to crops or to the native vegetation itself, can aid to reduce PV panels soiling [32], which occurs in PV plants where the ground gap between panels rows is bare or with little vegetation (Altyeb et al. 2022) [33].

4. Conclusions

Once the data object of this study have been analysed, and the previous discussions carried out, the following conclusions can be drawn:

Satellite imagery can be used to determine the environmental impact of installing an utility-scale photovoltaic plant. This option is accessible to the general public, although the treatment of the images and their interpretation requires some training and significant associated work.

After the installation of a photovoltaic plant, a decrease in moisture levels is observed in the area occupied by the plant, compared to the moisture levels in the areas distant from the PV plant. This decrease is also reflected in the vegetation indices, although in this case it is less pronounced. According to our results, a weighted moderate decrease in both NDMI (-5%) and NDVI (-3%), compared to the distant areas, was detected after the solar plant installation.

The grade or slope of the terrain whereon the PV plant is installed plays an important role on its impact on the general moisture content, and it also affects vegetation indices. It is recommended to adopt mitigating measures in the case of photovoltaic installations on rough hilly terrains. Presumably, the rain and/or cleaning water that drains from the panels has a negative impact on the soil.

The use of solar trackers did not have a significant impact compared to plants that do not implement solar tracking. Both NDVI and NDMI indices were not significantly affected after the installation of solar tracking PV plants, compared to plants with fix-tilt PV panels.

The coexistence of photovoltaic plants and agriculture could mitigate the impact on the soil and would improve land use in the concept of Ground-Integrated Photovoltaics.

CRediT authorship contribution statement

Miguel-Ángel Muñoz-García: Methodology, Data curation, Investigation, Writing – original draft. **Luis Fialho:** Methodology, Project administration, Resources, Writing – review & editing. **Guillermo P. Moreda:** Validation, Investigation, Writing – review & editing. **Fátima Baptista:** Project administration, Resources, Writing – review & editing.

Declaration of competing interest

The authors declare that they have no known competing financial interests or personal relationships that could have appeared to influence the work reported in this paper.

Acknowledgments

The work presented has been co-funded by 'Programa Propio de Movilidad 2023' of Universidad Politécnica de Madrid in cooperation with Banco Santander.

Annex I.

The 13 spectral bands of SENTINEL-2 range from the Visible (VNIR) and Near Infra-Red (NIR) to the Short Wave Infra-Red (SWIR):

- 4 × 10 metre Bands: the three classical RGB bands ((Blue (~493 nm), Green (560 nm), and Red (~665 nm)) and a Near Infra-Red (~833 nm) band;
- 6 × 20 metre Bands: 4 narrow Bands in the VNIR vegetation red edge spectral domain (~704 nm,~740 nm, ~783 nm and ~ 865 nm) and 2 wider SWIR bands (~1610 nm and ~ 2190 nm) for applications such as snow/ice/cloud detection, or vegetation moisture stress assessment;
- 3 × 60 metre Bands mainly focused towards cloud screening and atmospheric correction (~443 nm for aerosols and ~ 945 nm for water vapour) and cirrus detection (~1374 nm).

Table A1
10 m Spatial Resolution Bands and associated Signal to Noise ratio (SNR).

Band number	S2A		S2B		Lref (reference radiance)(W m−2 sr−1 μm−1)	SNR @ Lref
	Central wavelength (nm)	Bandwidth (nm)	Central wavelength (nm)	Bandwidth (nm)		
2	492.7	65	492.3	65	128	154
3	559.8	35	558.9	35	128	168
4	664.6	30	664.9	31	108	142
8	832.8	105	832.9	104	103	174

Table A2
20 m Spatial Resolution Bands and associated Signal to Noise ratio (SNR).

Band number	S2A		S2B		Lref (reference radiance) (W m−2 sr−1 μm−1)	SNR @ Lref
	Central wavelength (nm)	Bandwidth (nm)	Central wavelength (nm)	Bandwidth (nm)		
5	704.1	14	703.8	15	74.5	117
6	740.5	14	739.1	13	68	89

(*continued on next page*)

Table A2 (*continued*)

Band number	S2A		S2B		Lref (reference radiance) (W m−2 sr−1 μm−1)	SNR @ Lref
	Central wavelength (nm)	Bandwidth (nm)	Central wavelength (nm)	Bandwidth (nm)		
7	782.8	19	779.7	19	67	105
8a	864.7	21	864.0	21	52.5	72
11	1613.7	90	1610.4	94	4	100
12	2202.4	174	2185.7	184	1.5	100

Table A3
60 m Spatial Resolution Bands and associated Signal to Noise ratio (SNR).

Band number	S2A		S2B		Lref (reference radiance) (W m−2 sr−1 μm−1)	SNR @ Lref
	Central wavelength (nm)	Bandwidth (nm)	Central wavelength (nm)	Bandwidth (nm)		
1	442.7	20	442.2	20	129	129
9	945.1	19	943.2	20	9	114
10	1373.5	29	1376.9	29	6	50

References

[1] Eurostat, Electricity production capacities for renewables and wastes, 2023.
[2] International Energy Agency, Outlook for electricity, 2022.
[3] International Energy Agency, Electricity Market Report 2023, 2023.
[4] A. Scognamiglio, Photovoltaic landscapes': design and assessment. A critical review for a new transdisciplinary design vision, Renew. Sustain. Energy Rev. (2016) 629–661.
[5] C. Dupraz, H. Marrou, G. Talbot, L. Dufour, A. Nogier, Y. Ferard, Combining solar photovoltaic panels and food crops for optimising land use: Towards new agrivoltaic schemes, Renewable Energy 36 (10) (2011) 2725–2732.
[6] M.R. E, et al., Agrivoltaic systems potentials in Sweden: a geospatial-assisted multi-criteria analysis, Appl. Energy 356 (2024) 122108.
[7] R. B, et al., Realising co-benefits for natural capital and ecosystem services from solar parks: a co-developed, evidence-based approach, Renew. Sustain. Energy Rev. 125 (2020) 109775.
[8] A.L.S. Hu, G. Meehl, W. Han, W. Washington, K. Oleson, et al., Impact of solar panels on global climate, Nat. Clim. Change 6 (2016) 290–294.
[9] D. Millstein, S. Menon, Regional climate consequences of large-scale cool roof and photovoltaic array development, Environ. Res. Lett. 6 (2011) 034001.
[10] C, et al., A coupled WRF-PV mesoscale model simulating the near-surface climate of utility-scale photovoltaic plants, Sol. Energy 245 (2022) 278–289.
[11] G. Barron-Gafford, R. Minor, N. Allen, A. Cronin, A. Brooks, M. Pavao-Zuckerman, The photovoltaic heat island effect: Larger solar plants increase local temperatures, Sci. Rep. 6 (2016) 35070.
[12] A. Broadbent, E. Krayenhoff, M. Georgescu, D. Sailor, The observed effects of utility-scale photovoltaics on near-surface air temperature and energy balance, J. Appl. Meteorol. Clim. 58 (2019), 989-06.
[13] W, et al., Ecohydrological effects of photovoltaic solar farms on soil microclimates and moisture regimes in arid Northwest China: a modeling study, Sci. Total Environ. 802 (2022) 149946.
[14] Y, et al., Minimizing environmental impacts of solar farms: a review of current science on landscape hydrology and guidance on stormwater management, Environ. Res. Infrastruct. Sustain. 2 (2022) 032002.
[15] A, et al., Solar park microclimate and vegetation management effects on grassland carbon cycling, Environ. Res. Lett. 11 (2016) 074016.
[16] C, et al., Environmental co-benefits of maintaining native vegetation with solar photovoltaic infrastructure, Earth's Future 11 (2023) e2023EF003542.
[17] K, et al., Grassland carbon-water cycling is minimally impacted by a photovoltaic array, Commun. Earth Environ. 4 (2023) 238.
[18] L, et al., Climate model shows large-scale wind and solar farms in the Sahara increase rain and vegetation, Science 361 (2018) 1019.
[19] G, et al., Ground-mounted photovoltaic solar parks promote land surface cool islands in arid ecosystems, Renew. Sustain. Energy Transit. 1 (2021) 100008.
[20] A.E.D.K.Y. Abdullah Demir, A novel method for the site selection of large-scale PV farms by using AHP and GIS: a case study in İzmir, türkiye, Sol. Energy 259 (2023) 235–245.
[21] Z, et al., Mapping photovoltaic panels in coastal China using Sentinel-1 and Sentinel-2 images and Google Earth engine, Remote Sensing 15 (2023) 3712.
[22] C. Buerhop, L. Bommes, J. Schlipf, T. Pickel, A. Fladung, I. M. Peters, Infrared imaging of photovoltaic modules: a review of the state of the art and future challenges facing gigawatt photovoltaic power stations, Progr. Energy, 4 (2022).
[23] C. Jörges, H. S. Vidal, T. Hank, H. Bach, Detection of Solar Photovoltaic Power Plants Using Satellite and Airborne Hyperspectral Imaging, *Remote Sensing,* 15 (2023).
[24] C. Fan, X. Huang, Direct impact of solar farm deployment on surface longwave radiation, Environ. Res. Commun., 3 (2021) 125006.
[25] H, et al., Impact of a small-scale solar park on temperature and vegetation parameters obtained from Landsat 8, Renewable Energy 221 (2024) 119827.
[26] X, et al., A global assessment of the effects of solar farms on albedo, vegetation, and land surface temperature using remote sensing, Solar Energy 268 (2024) 112198.
[27] X, et al., Solar photovoltaic program helps turn deserts green in China: evidence from satellite monitoring, J. Environ. Manag. 324 (2022) 116338.
[28] B-M, et al., A fast operative method for NDVI uncertainty estimation and its role in vegetation analysis, Eur. J. Remote Sensing 49 (2016) 137–156.
[29] S.S. F, B.-M.E. De Petris, Uncertainty assessment of Sentinel-2-retrieved vegetation spectral indices over Europe, Eur. J. Remote Sensing (2023) 2267169.
[30] P. Jain, G. Raina, S. Sinha, P. Malik, S. Mathur, Agrovoltaics: step towards sustainable energy-food combination, Bioresour. Technol. Rep. 15 (2021) 100766.
[31] M.A. Muñoz-García, L. Hernández-Callejo, Photovoltaics and electrification in agriculture, MDPI (2022).
[32] T.F.E.P. Miguel-Ángel Muñoz-García, Analysis of the soiling effect under different conditions on different photovoltaic glasses and cells using an indoor soiling chamber, Renewable Energy 163 (2021) 1560–1568.
[33] E.A. Altyeb Ali Abaker Omer, Water evaporation reduction by the agrivoltaic systems development, Solar Energy 247 (2022) 13–23.